

Numerical analysis of microchannel heat sink composed of SiC and CNT reinforced ZrB₂ composites

DOI : 10.36909/jer.18359

Akash Dwivedi*, Mohammad Mohsin Khan*, Harveer Singh Pali*

*Mechanical Engineering Department, National Institute of Technology, Srinagar

*Corresponding Author: mohsinkhan@nitsri.ac.in

ABSTRACT

As a result of the development of micro-electro-mechanical systems (MEMS), it is now feasible to achieve enormous heat transfer, even though electrical and electronic devices have more compact spaces. A heat sink is a device that collects significant amounts of heat from various electrical and electronic surfaces and then releases that heat into the surrounding environment. In the current study, a ceramic microchannel heat sink (MCHS) with a rectangular channel having a length of 10 mm and dimensions of 57×180 μm was investigated numerically. Because ceramics are valuable materials that can withstand corrosive environments and extreme temperatures, they are statistically analyzed to evaluate whether a substance can work under such harsh conditions. Firstly, the finite element approach was used to solve the governing equations of the solid domain as ZrB₂ composites and the fluid domain as water. Subsequently, a numerical analysis was conducted on an MCHS constructed from ZrB₂ composites reinforced with SiC and CNT in a variable proportion of 20 vol.% and 10 vol.%, respectively. The results reveal the most significant temperature reduction for an ultra-high heat flux for the ZrB₂ composite reinforced with 20 vol.% SiC, followed by the ZrB₂ composite reinforced with 20 vol.% SiC & 10 vol.% CNT at Reynolds number 250. The fundamental causes of the exceptional heat transfer rate are the high surface density of the microchannel and the excellent thermal conductivity of the UHTCs.

Keywords: ANSYS Workbench, Ceramic Materials, Heat sink, Microchannel, ZrB₂

Introduction

The high-power demand, lightweight and smaller size of modern electronic devices have

pushed toward finding efficient and compact heat sinks for removing ultra-heat fluxes. Because high temperatures might cause these electronic devices to malfunction, therefore the operating temperature for these electronic devices must be maintained below 403 K for stable and efficient performance (Fedorov and Viskanta, **2000**). Because, logically, narrower channel diameters promote higher heat transfer and smaller unit sizes, the application and utilization of narrow flow channels have recently gained attention. Recent advances in micro-fabrication and micro-miniaturization processes have enabled the machining of narrow flow passages or 'microchannels'. Microchannels are defined as narrow flow channels of 1mm or less in diameter, allowing high surface densities of 10000 m²/m³ or more; which is exceptionally high when compared to conventional heat exchangers with a surface density of 700 m²/m³. "Tuckerman and Pease" was a founder of the MCHS. They created a small water-cooled silicon microchannel heat sink that could absorb 790 W/cm² of heat while keeping the heated region at 71°C(Tuckerman and Pease, **1981**).

Additionally, the thermal performance of MCHS can be enhanced mainly by active and passive techniques (Kandlikar and Grande, **2003**). External forces such as magnetic flux, electric flux, and vibrational forces are employed in active techniques to promote heat transfer. In the passive technique, instead of using external forces, heat transfer is generally improved by using various flow disruption methods, changes in geometry and changes in the working fluid of the heat sink.(Mohammed, Gunnasegaran and Shuaib, **2011**) investigated the heat flow behaviour of wavy microchannel heat sinks with rectangular geometry and wave amplitudes varying from 125 m to 500 m. They found that enhanced heat transfer could be achieved compared to a straight microchannel by utilizing a wavy microchannel. In the transverse microchambers, Chai et al. (Chai and Wang, **2018**) examined the thermo-fluidic behaviour of an interrupted MCHS using various rib configurations. Their results suggest that employing ribs improves the thermal characteristics of Microchannels. In another study (Ghani, Kamaruzaman and Sidik, **2017**) analyze the thermo-fluidic behaviour of a microchannel heat sink for 100 to 800

Reynolds numbers having sinusoidal cavities & rectangular ribs (MC-SCRR) was investigated. According to the results in terms of thermal performance, MC-SCRR surpasses both channels with sinusoidal cavities and rectangular ribs.

Moreover, (Feng *et al.*, **2017**) investigated the heat transfer in MCHS by incorporating wire coils in a numerical investigation. Their outcomes demonstrate that longitudinal vortexes generated by wire coils increase the heat transfer in the MCHS, but the flow resistance also increases simultaneously. In another study, (Heidarshenas *et al.*, **2021**) used an ionic liquid- Al_2O_3 hybrid nanofluid to investigate the thermo-fluidic behaviour in a cylindrical MCHS. According to the findings, the Ionic liquid-alumina hybrid nanofluid increased the Nusselt number by up to 40%. By utilizing nanofluids & swirl flow (Ali *et al.*, **2021**) examines the thermo-fluidic characteristics of circular MCHS and demonstrate that by using nanofluids & swirl flow, the thermal resistances of microchannels can be reduced. By changing the construction material of the MCHS, the thermal performance of the heat sink can be further increased (Sarafraz *et al.*, **2018**). Because the thermal performance of good conductors of heat is high, materials with high thermal conductivity should be used to construct a heat sink (Zhou *et al.*, **2019**). However, they should continue to function in their current forms and structure at high heat fluxes. Metals and their alloys are commonly used for heat exchanger construction owing to their high thermal conductivity; however, their performance has been limited because of their low corrosion resistance and metal deformation at high temperatures. Ultra-high temperature ceramic materials (UHTC) can be a good substitute for these conditions (Vajdi, Sadegh Moghanlou, *et al.*, **2020**) (Sahar Nekahi *et al.*, **2019**) (S. Nekahi *et al.*, **2019**) (Vajdi, Shahedi Asl, *et al.*, **2020**) (Fattahi *et al.*, **2020**). UHTC is a collection of materials with substantially high melting points & resilience that offer outstanding physical and chemical stability at elevated temperatures (Sadegh Moghanlou *et al.*, **2019**).

As a member of the UHTC family, zirconium diboride (ZrB_2) possesses exceptional thermal & mechanical properties, including high hardness, high melting point (3529 K), high Young's modulus of elasticity (520 MPa), & exceptional thermal conductivity (55–140 W/m-K). Thus,

ZrB₂ is an appropriate material for severe working environments, such as abrasion, shock, corrosion, wear, and high temperatures. However, ZrB₂ as a member of UHTC, possesses insufficient oxidation resistance at higher temperatures, particularly above 2000°C. To overcome this deficiency, SiC, typically between 10 and 30 vol.%, is reinforced to obtain a covering of SiO₂ during the oxidization in UHTC (Shahedi Asl *et al.*, **2019**). Whereas to improve the flexural strength of ZrB₂, CNT is added (Nisar *et al.*, **2019**). There is little research has been conducted on UHTC in MCHS based on the abovementioned qualities and applications. Because numerical analysis allows for a more realistic image of the heat flow behaviour of fluids within the MCHS, most studies currently employ numerical approaches (Gök, **2017**; Gök, Selçuk and Gök, **2021**; Gok, **2022**)(Pirhan, Gök and Gök, **2020**). Thus, the primary goal of this study is to perform a computational analysis on the thermo-fluidic behaviour of a ZrB₂ composite MCHS reinforced with SiC and CNT to assess its suitability for use in electronic components. This study employs a finite element approach to evaluate the heat sink behaviour under actual working conditions.

Geometry of the microchannel heat sink

The device examined was an MCHS on which an electronic component was placed. The geometry of the MCHS is based on the set-up presented by (Bhattacharya, Samanta and Chakraborty, **2009**), which was used as the basis in the present study. The heat sink has a rectangular channel with a length of 10 mm and dimensions of 57×180 μm. Channels were fabricated from ZrB₂ composites reinforced with SiC & CNT. Fig. 1 show the 3-D perspectives of an MCHS & a detailed assessment of the channel with boundary conditions. Because of the identical heat transfer behaviour of all the MCHS channels, one of the channels was selected and considered as a computational fluid domain for simulation instead of examining all the channels.

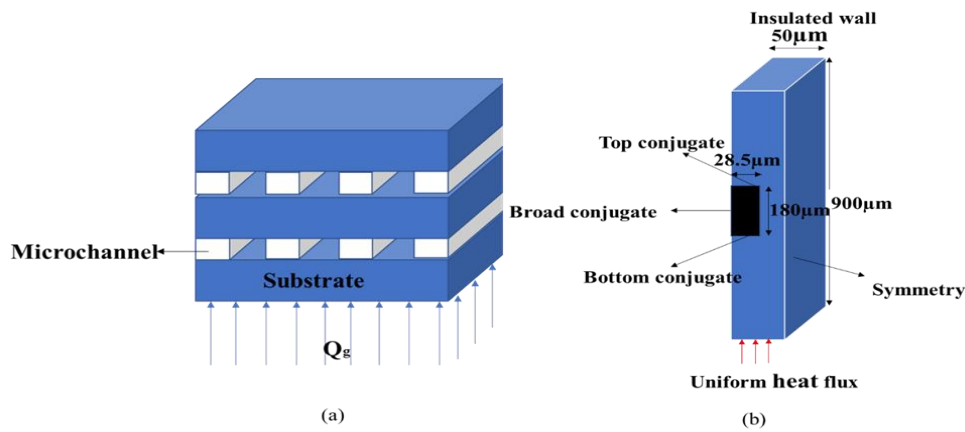


Fig. 1 MCHS geometry & boundary conditions. (a) front view (b) detailed view

Governing equations & Numerical approach

Simulations of the MCHS with rectangular geometry made from ZrB_2 composites and reinforced with SiC & CNT were carried out in ANSYS using the fluent module. An electronic component is placed on the heat sink's base surface. The heat produced by electronic gadgets is transmitted to the channels via conduction through the solid. The coolant then dissipates heat through the channels. The working fluid, steady-state continuity equation, and conservation equations for momentum & energy were solved. However, for a solid, the steady-state conduction equation is solved. Equations 1 through 4 provide the entire range of governing equations necessary for solving this three-dimensional conjugate heat transfer.

Conservation of mass equation:

$$\rho \nabla \cdot (\mathbf{V}) = 0 \quad (1)$$

Where ∇ & \mathbf{V} are Nabla mathematical operator & velocity vector respectively.

Conservation of momentum equation:

$$\rho_f \mathbf{v} \cdot \nabla \mathbf{v} = -\nabla p + \nabla \cdot (\mu_f \nabla \mathbf{v}) \quad (2)$$

Where ρ_f , p and μ_f are the density, pressure, and viscosity, respectively of the fluid.

Conservation of energy equation for working fluid:

$$\rho_f C_{pf} \nabla T = \nabla \cdot (k_f \nabla T) \quad (3)$$

where C_{pf} , T and k_f is the specific heat, temperature and thermal conductivity, respectively of

the fluid.

Conservation of Energy equation for solid

$$\nabla \cdot (k_s \nabla T) = 0 \quad (4)$$

Where k_s is the thermal conductivity of solid.

Thermal resistance equation

Thermal resistance contains 3 components: capacity resistance, conductivity, and convection.

$$R_{\text{total}} = R_{\text{conduction}} + R_{\text{capacity}} + R_{\text{convection}} \quad (5)$$

$$R_{\text{conduction}} = \frac{H}{KA} \quad (6)$$

$$R_{\text{convection}} = \frac{T_w - T_m}{Q} - R_{\text{conduction}} \quad (7)$$

$$R_{\text{capacity}} = \frac{T_w - T_m}{Q} \quad (8)$$

The thickness of the heat sink is H, where A is the area exposed for heat transfer, and Q is the heat energy. As Eq. (9), the total thermal strength can be calculated:

$$R_{\text{total}} = \frac{T_w - T_m}{Q} \quad (9)$$

Boundary conditions & Solution methodology

Water served as the working fluid in the microchannel, and the temperature at the microchannel entry was set at $T_0=293\text{K}$. On the bottommost surface of the heat sink, a consistent heat flow of $Q_g = 3.6 \times 10^6 \text{ W/m}^2$ was applied while the upper surface was isolated. The materials were defined based on the property functions generated, and the fluid regime was laminar with a Reynolds No. of 250. A constant mass flow rate based on a Reynolds No. of 250 was the entrance limit, while the atmospheric pressure was the exit limit. The entrance temperature was 293 K, and the limiting requirements for the heat transfer outflow of the fluid exiting the conduits were evaluated. The properties of the ZrB_2 composites reinforced with SiC & CNT were obtained from the literature (Nisar *et al.*, 2017).

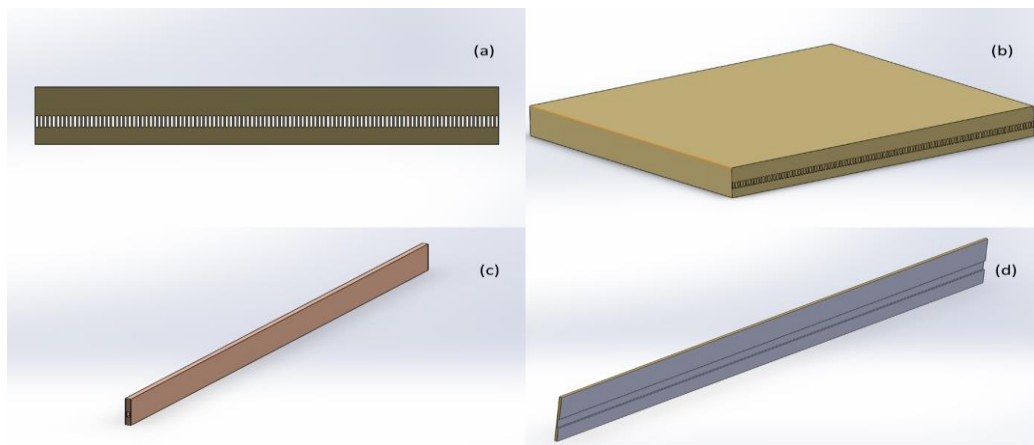


Fig. 2 (a) Front view of complete MCHS, (b) orthographic view of complete MCHS, (c) orthographic view and (d) cross-sectional view of an element of microchannel.

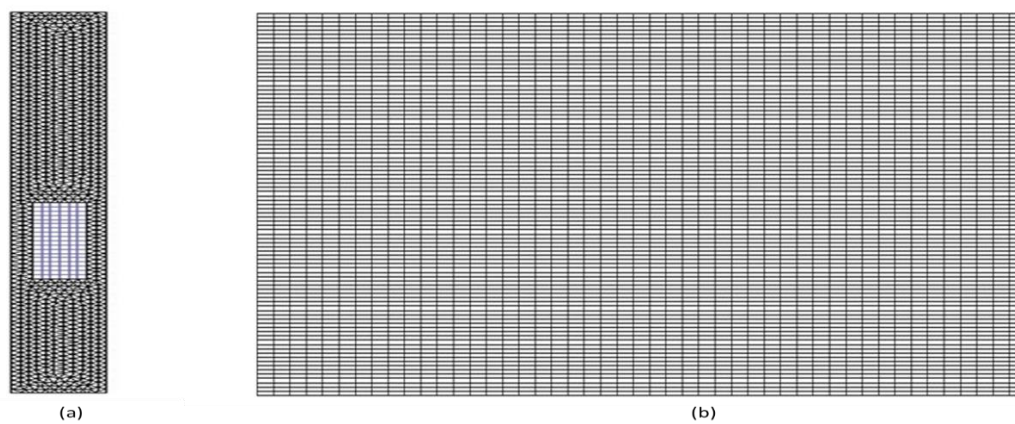


Fig. 3 Mesh view of microchannel element (a) front (b) side

The governing equations 1 to 4 and the boundary conditions discussed in section 4 were calculated by the finite element method using the ANSYS fluent module. The model was divided into two main domains solid and fluid. Fig. 2 illustrates the cross-section of the model. The flow geometry of the microchannel was split into minute pieces known as elements, and the corner of all elements was known as a node. These elements and nodes form a mesh/grid. This method is known as meshing. The grid development includes characterizing the structure and geometry and producing a grid on that geometry afterwards. The total number of meshed elements generated was 3,65,600. A Mesh view of the channel element is shown in Fig. 3.

Results and discussion

To investigate the effects of ZrB_2 composites reinforced with SiC and CNT MCHS on the

thermal performance of electronic gadgets, several computational simulations were performed. Simulations were performed on the geometry used by Bhattacharya et al. Identical geometries and materials were used to validate the results, as they had done in their report. A comparison analysis at Reynolds No. =250 and $Q_g = 0.9 \times 10^6 \text{ W/m}^2$ shows excellent consistency with the experimental results of Bhattacharya et al. (Bhattacharya, Samanta and Chakraborty, **2009**). As a result, the current simulation strategy analyses the temperature contour, pressure drop and convection coefficient of the MCHS composed of ZrB_2 composites, ZrB_2 reinforced with 20 vol.% SiC composites, ZrB_2 reinforced with 10 vol.% CNT composites, and ZrB_2 reinforced with 20 vol.% SiC & 10 vol.% CNT composites.

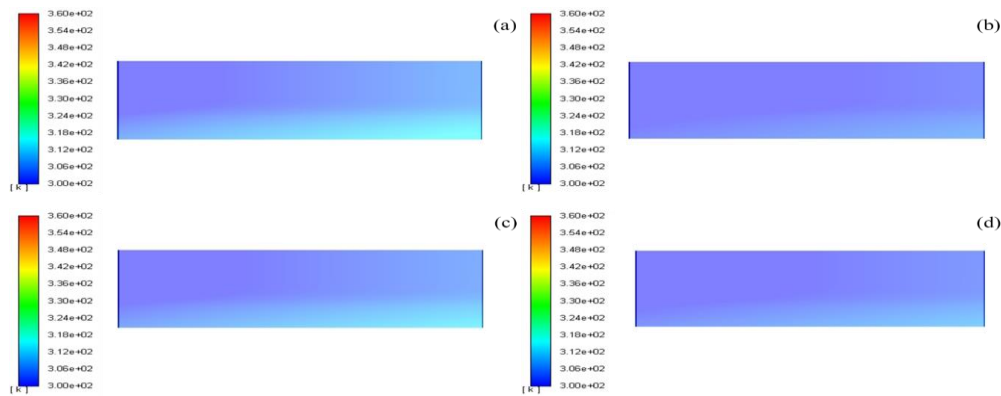


Fig. 4 Wall temp. contour of different material at Reynolds no.= 250 and heat flux $Q_g = 0.9 \times 10^6 \text{ W/m}^2$ (a) ZrB_2 (b) ZrB_2 -20 vol.% SiC (c) ZrB_2 -10 vol.% CNT & (d) ZrB_2 -20 vol.% SiC

Temperature profiles of four distinct composite materials subjected to a heat flux $Q_g = 0.9 \times 10^6 \text{ W/m}^2$ and a Reynolds No. of 250 are shown in Fig. 4 (a), (b), (c) & (d) respectively. The results demonstrate that the minimum temperature in the heat sink among all the composites was for ZrB_2 reinforced with 20 vol.% SiC. In addition, with an increase in the length of the channel, the heat sinks temperature increases. This occurs because as the working fluid advances toward the exit surface, the temperature gradient between the working fluid and the electronic component diminishes.

Fig. 5(a), (b), (c) & (d) represent the temperature profiles of ZrB_2 composites reinforced with SiC & CNT microchannel heat sinks, respectively at heat flux $Q_g = 1.8 \times 10^6$. From the

temperature contours of the various composites, it can be observed that with the increase in heat generation, the minimum temperature of the MCHS increases for all the composites. However, among them, ZrB₂ reinforced with 20 vol.% SiC has the minimum temperature.

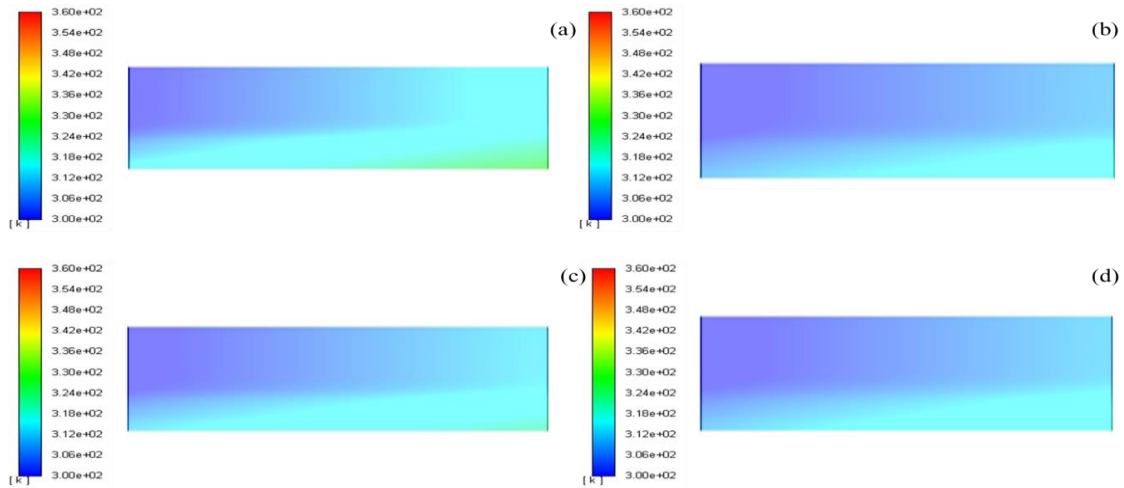


Fig. 5 Wall temp. contour of different material at Reynolds No.= 250 and heat flux $Q_g = 1.8 \times 10^6$ W/m² (a) ZrB₂ (b) ZrB₂-20 vol.% SiC (c) ZrB₂-10 vol.% CNT & (d) ZrB₂-20 vol.% SiC

Because the maximum wall temperature of the MCHS increases with increasing heat generation, knowing the maximum wall temperature of the MCHS for higher heat generation is significant. Therefore, further simulations were performed at higher heat fluxes. Fig. 6 shows the temperature profiles of ZrB₂ composites reinforced with SiC and CNT MCHS at $Q_g = 2.7 \times 10^6$ W/m² and Reynolds No. = 250. While Fig. 7 shows the temperature contours of ZrB₂ composites reinforced with SiC and CNT at $Q_g = 3.6 \times 10^6$ W/m² and Reynolds No. = 250. The results demonstrate that the minimum wall temperature among all the composites is for ZrB₂ reinforced with 20 vol.% SiC at different heat fluxes.

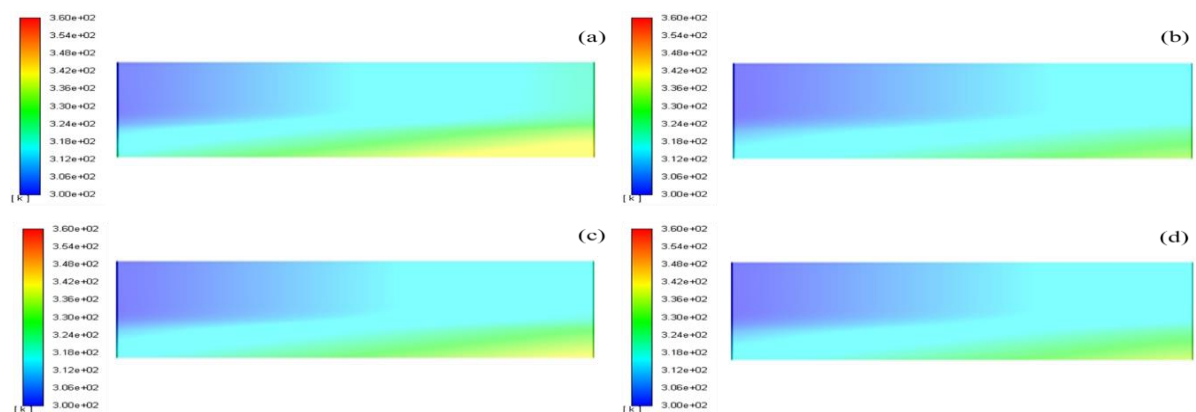


Fig. 6 Wall temp. contour of different material at Reynolds No.= 250 and heat flux $Q_g = 2.7 \times 10^6$ W/m² (a) ZrB₂ (b) ZrB₂-20 vol.% SiC (c) ZrB₂-10 vol.% CNT & (d) ZrB₂-20 vol.% SiC

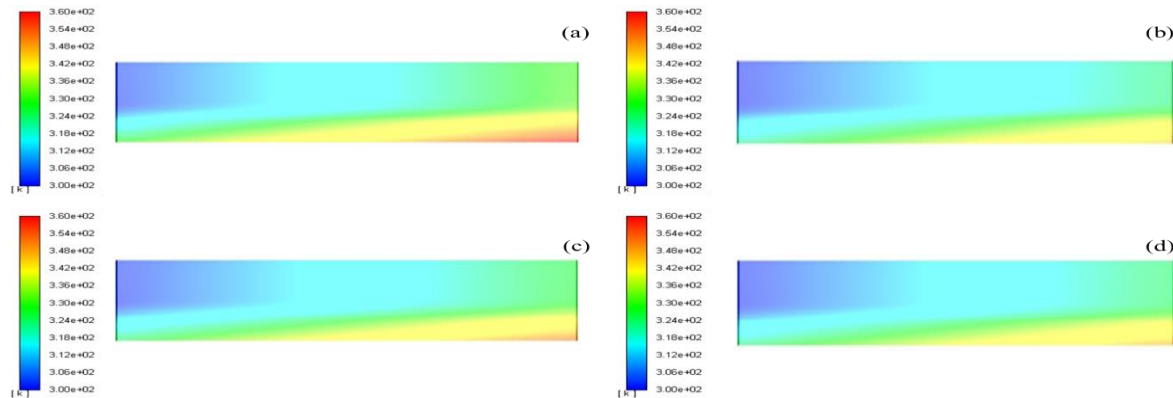


Fig. 7 Wall temp. contour of different material at Reynolds No.= 250 and heat flux $Q_g = 3.6 \times 10^6$ W/m² (a) ZrB₂ (b) ZrB₂-20 vol.% SiC (c) ZrB₂-10 vol.% CNT & (d) ZrB₂-20 vol.% SiC

Wall temperature for different materials at Reynolds No. = 250 and different heat fluxes is shown in Fig. 8. The results demonstrate that for all the different heat flux values among the four composite materials, the minimum temperature drop in the ZrB₂ reinforced with 20 vol.% SiC followed by ZrB₂ reinforced with 20 vol.% SiC and 10 vol.% CNT. In addition, compared with the top and bottom surfaces of the heat sink, the temperature of the bottom surface of the sink is maximum because this is the location where the heat flux of the electronic component is applied. It's noteworthy to note that for ZrB₂ reinforced with 20 vol.% SiC at a heat flow of 0.9 MW/m^2 , the highest temperature of the surface of an electronic component does not reach 307 K. The high heat transfer area to the occupied volume is the cause of ultra-high heat flux absorption of microchannels. One of the most appealing features of UHTC MCHS is its ability to cool hot surfaces quickly due to its higher thermal conductivity. The results also show that at a high flux of $3.6 \times 10^6 \text{ W/m}^2$, the maximum wall temperature is 348 K only. This value is much lower than the safe operating temperature for electronic components as reported in the literature (Fedorov and Viskanta, 2000).

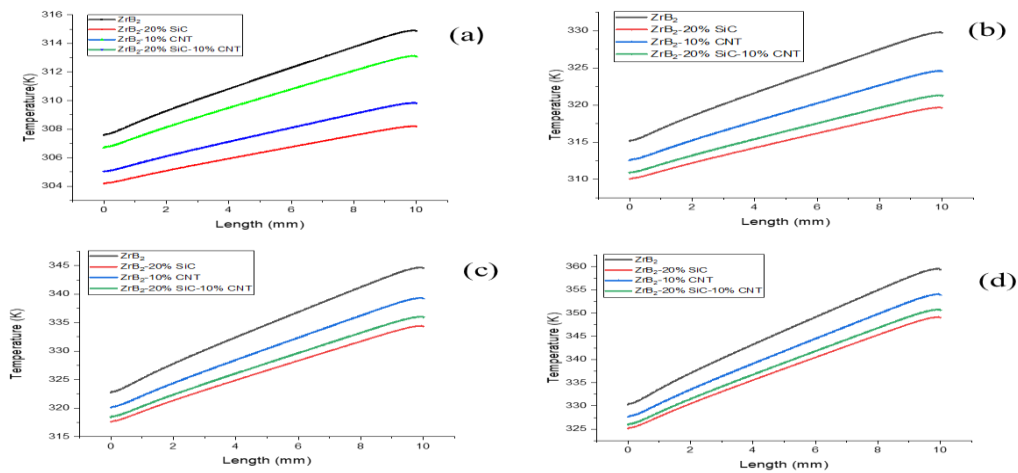


Fig. 8 Wall Temperature of different materials at Reynolds No. of 250 (a) at heat flux of $Q_g = 0.9 \times 10^6 \text{ W/m}^2$ (b) $Q_g = 1.8 \times 10^6 \text{ W/m}^2$ (c) $Q_g = 2.7 \times 10^6 \text{ W/m}^2$ & (d) $Q_g = 3.6 \times 10^6 \text{ W/m}^2$

Fig. 9(a) represents the convective heat transfer coefficient for ZrB_2 composites reinforced with SiC & CNT at various Reynolds numbers. The obtained findings suggest that ZrB_2 reinforced with 20 vol.% SiC has the highest heat transfer coefficient, followed by ZrB_2 reinforced with 20 vol.% SiC & 10 vol.% CNT respectively. According to fig, there is a significant convective heat transfer coefficient at all Reynolds numbers. Since Reynolds No. is directly proportional to the fluid velocity. Therefore, as Reynolds No. increases, fluid velocity increases and hence heat transfer coefficient increases.

Pressure drop is another aspect of the fluidic system that exposes the necessity of pumping effort to circulate the working fluid. Fig. 9(b) shows the drop-in pressure for an MCHS composed of ZrB_2 composites at different Reynolds numbers. The results revealed that ZrB_2 reinforced with 20 vol.% SiC seemed to have the highest pressure drop. There is a drop-in pressure of almost 1.74 bar at Reynolds No.=250 for the ZrB_2 reinforced with 20 vol.% SiC composite. This indicates a very high-pressure drop in the MCHS. The results show that there is a considerable pressure drop for all the composites. As the Reynolds No. climbs, this value rises tremendously. This is due to the micro size of the Microchannels. Microchannels generally experience considerable pressure drop, which is a challenge when using them.

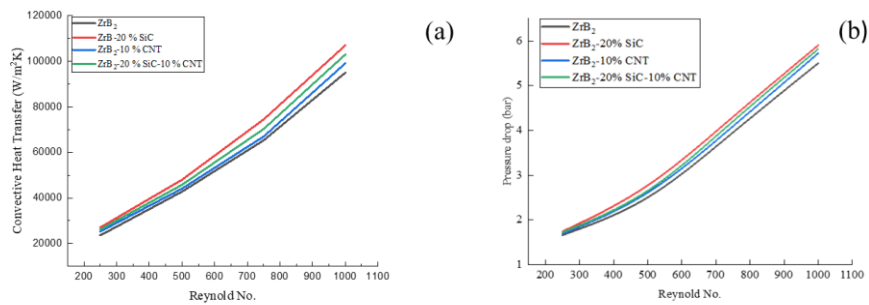


Fig.9 (a) Convective heat transfer for various Materials versus Reynolds No. (b) Pressure drop for various microchannel materials versus Reynolds No..

Conclusions

ZrB₂ composites have fascinating thermal and high strength qualities as ultrahigh temperature ceramics. Micro-channels offer remarkable heat transfer properties, allowing them to absorb extremely high heat fluxes in minimal regions. In order to investigate a heat sink made up of composites of ZrB₂ reinforced with SiC & CNT at very high heat flow, the finite element methodology was applied. The composite reinforced with 20 vol.% SiC shows the lowest wall temperature at a high heat flux $Q_g = 3.6 \times 10^6 \text{ W/m}^2$ and Reynolds No. = 250. The reason for this ultra-high heat flux absorption is the enormous heat transfer area to volume ratio of microchannels compared to conventional devices and the high thermal conductivity of UHTC. According to these observations, the ZrB₂ reinforced with 20 vol.% SiC has the best heat transfer coefficient. However, the results also revealed that a material consisting of ZrB₂ reinforced with 20 vol.% SiC had the maximum pressure drop, which is a challenge of employing microchannels, but an increase in heat transfer compensates for this value.

REFERENCES

- Ali, A.M. et al. (2021)** ‘Thermo-hydraulic performance of a circular microchannel heat sink using swirl flow and nanofluid’, *Applied Thermal Engineering*, 191, p. 116817.
- Bhattacharya, P., Samanta, A.N. and Chakraborty, S. (2009)** ‘Numerical study of conjugate heat transfer in rectangular microchannel heat sink with Al₂O₃/H₂O nanofluid’,

Heat and Mass Transfer/Waerme- und Stoffuebertragung, 45(10), pp. 1323–1333.

Chai, L. and Wang, L. (2018) ‘Thermal-hydraulic performance of interrupted microchannel heat sinks with different rib geometries in transverse microchambers’, *International Journal of Thermal Sciences*, 127, pp. 201–212.

Fattahi, M. et al. (2020) ‘Aluminum nitride as an alternative ceramic for fabrication of microchannel heat exchangers: A numerical study’, *Ceramics International*, 46(8), pp. 11647–11657.

Fedorov, A.G. and Viskanta, R. (2000) ‘Three-dimensional conjugate heat transfer in the microchannel heat sink for electronic packaging’, *International Journal of Heat and Mass Transfer*, 43(3), pp. 399–415.

Feng, Z. et al. (2017) ‘Numerical investigation on laminar flow and heat transfer in rectangular microchannel heat sink with wire coil inserts’, *Applied Thermal Engineering*, 116, pp. 597–609.

Ghani, I.A., Kamaruzaman, N. and Sidik, N.A.C. (2017) ‘Heat transfer augmentation in a microchannel heat sink with sinusoidal cavities and rectangular ribs’, *International Journal of Heat and Mass Transfer*, 108, pp. 1969–1981.

Gök, A. (2017) ‘2D numeric simulation of serrated-chip formation in orthogonal cutting of AISI316H stainless steel’, *Materiali in Tehnologije*, 51(6), pp. 953–956.

Gok, A. (2022) ‘Design and Numerical Analysis Of Face Mask Polymer Shield Against Infectious Diseases’, *Journal of Mechanics in Medicine and Biology* [Preprint].

Gök, K., Selçuk, A.B. and Gök, A. (2021) ‘Computer-Aided Simulation Using Finite Element Analysis of Protect Against to Coronavirus (COVID-19) of Custom-Made New Mask Design’, *Transactions of the Indian Institute of Metals*, 74(5), pp. 1029–1033.

Heidarshenas, A. et al. (2021) ‘Experimental investigation of heat transfer enhancement using ionic liquid-Al₂O₃ hybrid nanofluid in a cylindrical microchannel heat sink’, *Applied*

Thermal Engineering, 191, p. 116879.

Kandlikar, S.G. and Grande, W.J. (2003) ‘Evolution of microchannel flow passages-thermohydraulic performance and fabrication technology’, *Heat Transfer Engineering*, 24(1), pp. 3–17.

Mohammed, H.A., Gunnasegaran, P. and Shuaib, N.H. (2011) ‘Numerical simulation of heat transfer enhancement in wavy microchannel heat sink’, *International Communications in Heat and Mass Transfer*, 38(1), pp. 63–68.

Nekahi, Sahar et al. (2019) ‘A numerical approach to the heat transfer and thermal stress in a gas turbine stator blade made of HfB₂’, *Ceramics International*, 45(18), pp. 24060–24069.

Nekahi, S. et al. (2019) ‘TiB₂–SiC-based ceramics as alternative efficient micro heat exchangers’, *Ceramics International*, 45(15), pp. 19060–19067.

Nisar, A. et al. (2017) ‘Effect of carbon nanotube on processing, microstructural, mechanical and ablation behavior of ZrB₂-20SiC based ultra-high temperature ceramic composites’, *Carbon*, 111, pp. 269–282.

Nisar, A. et al. (2019) ‘Processing, microstructure and mechanical properties of HfB₂ - ZrB₂ -SiC composites: Effect of B₄C and carbon nanotube reinforcements’, *International Journal of Refractory Metals and Hard Materials*, 81(February), pp. 111–118.

Pirhan, Y., Gök, K. and Gök, A. (2020) ‘Comparison of two different bowel anastomosis types using finite volume method’, *Computer methods in biomechanics and biomedical engineering*, 23(8), pp. 323–331.

Sadegh Moghanlou, F. et al. (2019) ‘A numerical approach to the heat transfer in monolithic and SiC reinforced HfB₂, ZrB₂ and TiB₂ ceramic cutting tools’, *Ceramics International*, 45(13), pp. 15892–15897.

Sarafraz, M.M. et al. (2018) ‘Thermal performance of a heat sink microchannel working

with biologically produced silver-water nanofluid: Experimental assessment', *Experimental Thermal and Fluid Science*, 91, pp. 509–519.

Shahedi Asl, M. et al. (2019) 'Investigation of hot pressed ZrB₂–SiC–carbon black nanocomposite by scanning and transmission electron microscopy', *Ceramics International*, 45(14), pp. 16759–16764.

Tuckerman, D.B. and Pease, R.F.W. (1981) 'High-Performance Heat Sinking for VLSI', *IEEE Electron Device Letters*, EDL-2(5), pp. 126–129.

Vajdi, M., Sadegh Moghanlou, F., et al. (2020) 'Heat transfer and pressure drop in a ZrB₂ microchannel heat sink: A numerical approach', *Ceramics International*, 46(2), pp. 1730–1735.

Vajdi, M., Shahedi Asl, M., et al. (2020) 'Numerical assessment of beryllium oxide as an alternative material for micro heat exchangers', *Ceramics International*, 46(11), pp. 19248–19255.

Zhou, F. et al. (2019) 'Heat transfer characteristics of Cu-based microchannel heat exchanger fabricated by multi-blade milling process', *International Journal of Thermal Sciences*, 138(January 2018), pp. 559–575.